

HOLOGRAPHIC DARK MATTER

Sylvain Fichet^{a *}, Eugenio Megías^{b †}, Mariano Quirós^{c ‡}

^a *CCNH, Universidade Federal do ABC, Santo Andre, 09210-580 SP, Brazil*

^b *Departamento de Física Atómica, Molecular y Nuclear and
Instituto Carlos I de Física Teórica y Computacional,
Universidad de Granada, Avenida de Fuente Nueva s/n, 18071 Granada, Spain*

^c *Institut de Física d'Altes Energies (IFAE) and
The Barcelona Institute of Science and Technology (BIST),
Campus UAB, 08193 Bellaterra, Barcelona, Spain*

Abstract

Cold dark matter may be a fluid (or plasma) residing in a strongly-interacting hidden sector, rather than a population of weakly-coupled particles. Such a scenario admits a holographic description in terms of a cosmological braneworld embedded in the linear dilaton five-dimensional (5D) spacetime. In this framework, dark matter originates from the linear dilaton bulk black hole, whose phase we show to be thermodynamically favored at all temperatures. We present a natural freeze-in mechanism for the production of holographic dark matter, in which the bulk black hole is fed by energy leaking from the brane after inflation. Our model is characterized by two free parameters, one of which, the position of the black hole horizon, is fixed by the observed dark matter abundance. The remaining parameter, the 5D Planck scale M_5 , is consistent with all current experimental bounds provided that $M_5 \gtrsim 3 \times 10^5$ TeV.

*sylvain.fichet@gmail.com

†emegias@ugr.es

‡quiros@ifae.es

Contents

1	Introduction	3
1.1	Comparison to the Literature	4
1.2	Outline	5
2	Holographic Fluids	5
2.1	The \mathcal{M}_ν Spacetimes	5
2.2	Physics on the Brane: Einstein Equation and Holographic Fluids	6
2.3	Thermodynamics of Holographic Fluids	7
3	Dark Matter as the $\nu = 1$ Holographic Fluid	8
3.1	Braneworld Cosmology and Friedmann Equations	8
3.2	Dark Matter as a Holographic Fluid	8
3.3	Holographic Dark Matter Thermodynamics	10
3.4	On the Model Parameters	12
4	Freeze-in Production of Holographic Dark Matter	12
4.1	Heating the Bulk: Graviton Radiation from the Brane	12
4.2	Evolution Equations: Boundary Viewpoint	13
4.3	Evolution Equations: Bulk Viewpoint	14
4.4	Initial Condition	15
4.5	Holographic Dark Matter Freeze-In	15
5	Phenomenological Constraints	18
5.1	Dark Matter Sound Speed	18
5.2	Supernovae Cooling	18
5.3	Big Bang Nucleosynthesis (BBN)	19
5.4	Deviation to Newtonian Potential	19
5.5	Discussion	20
6	Summary and Outlook	20
A	Computing Graviton Radiation from the Brane	21
A.1	Graviton Propagator	21
A.2	Bulk Graviton Emission	23

1 Introduction

Observations across all astronomical scales point to the existence of an unknown fluid permeating our Universe, commonly referred to as dark matter. The dominant view is that dark matter consists of a population of yet-unknown particles. A key assumption underlying this picture is that the hidden sector responsible for dark matter is *weakly coupled*. In this paper, building on our previous works [1, 2], we explore an alternative possibility: dark matter may instead be a fluid originating in a *strongly-coupled* hidden sector.¹

Our framework realizes a form of non-particle dark matter. Such a possibility has strong phenomenological motivation. Despite decades of increasingly sensitive experimental searches, no convincing signal of a dark matter particle has yet been observed. This depressing result motivates searching for a dark matter candidate that behaves as a pressureless fluid on astronomical scales, while remaining diffuse at microscopic scales to evade scattering with ordinary matter.

Remarkably, a candidate of this type arises naturally in string theory, in the so-called Little String Theory (LST) models [3, 4]. From the thermodynamics of LST, it can be inferred that LST behaves at finite temperature as a fluid with *vanishing pressure* [5, 6], which is precisely the macroscopic behavior we seek. Since LSTs are intrinsically strongly coupled, direct computations are challenging. However, a holographic description of LST has been known for a long time [7]. This description is based on the so-called *linear dilaton* (LD) spacetime, a simple background that appears in a variety of string-theoretic contexts. Roughly speaking, the relation between LD and LST plays a role analogous to that between AdS and CFT.

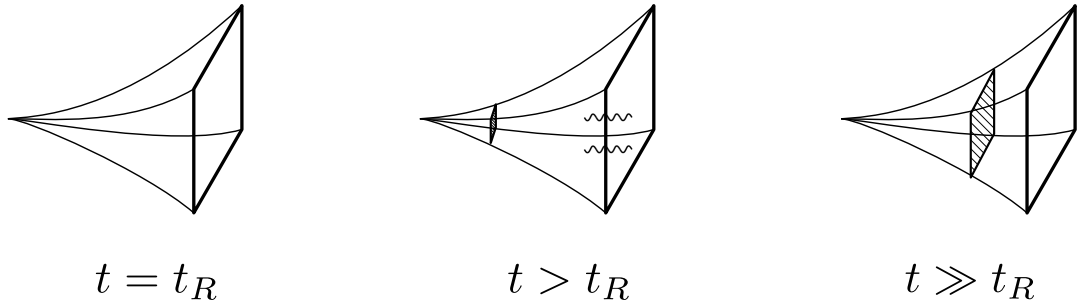
While having a string construction provides an excellent theoretical motivation, we do not need the string machinery to obtain a model of non-particle dark matter. Instead, it is sufficient to work with a consistent five-dimensional gravitational framework. In the minimal version which is our focus, the Standard Model (SM) fields are localized on a brane embedded in the 5D LD spacetime. This defines the cosmological LD₅ braneworld model, which is the framework explored in this work.

In this holographic description of dark matter, the pressureless fluid originates from a black hole living in the bulk spacetime. Our previous work [1, 2] already explored this fascinating phenomenon, which has a well-known AdS analog (see e.g. [8–10]). It is in fact instructive to contrast our setup with the minimal AdS₅ braneworld, namely the RS2 model [11]. In RS2 cosmology, the bulk black hole gives rise to a dark radiation component in the effective Friedmann equation, that may spoil predictions of Big Bang Nucleosynthesis [9, 12–15]). By contrast, in the LD₅ braneworld this unwanted dark radiation contribution is replaced by a desirable dark matter-like component. By changing the bulk geometry, we turn a fundamental drawback of braneworld cosmology into a virtue.

In this work we present the essential cosmological evolution of holographic dark matter. We show that a freeze-in mechanism naturally takes place, driven by interactions of the

¹The term *plasma* is also employed in the context of strongly-interacting theories.

SM with bulk gravitons. We assume that the inflaton couples only to SM fields. As a consequence, the dark sector has negligible energy density after inflation, i.e. the bulk black hole is nonexistent. Starting at the reheating time t_R , energy leaking from the brane feeds the bulk black hole, which grows until the emission rate becomes negligible. At later times, the horizon radius freezes. This holographic freeze-in mechanism can be schematically viewed as



At late times, the black hole contribution to the brane Friedmann equation simply redshifts as pressureless matter as the universe expands, eventually matching the observed dark matter abundance.

1.1 Comparison to the Literature

Let us emphasize the distinctions of the holographic dark matter framework with respect to some other proposals available in the literature.

First, the holographic model we propose is unrelated to the recent proposal [16] in which the behavior of the dark matter energy density is motivated from a bound inspired by the general holographic principle [17–21]. In a sense, our model relies on a concrete realization of the holographic principle — involving the LD₅ spacetime.

Second, although we assume a 4D strongly-interacting dark sector, our proposal is not a version of “dark QCD”. We do not assume that dark matter consists of a population of dark hadrons, which would bring us back to a weakly coupled effective field theory description below the (dark) confinement scale. See e.g. [22–26] for models in which dark matter is identified with dark hadrons. Along the same lines, both flat and warped five-dimensional scenarios feature weakly-coupled 4D Kaluza-Klein (KK) modes that have been considered as dark matter candidates, see e.g. [27–36]. While our holographic description of dark matter relies on a warped extra dimension, the specific geometry required (namely LD₅) does not produce isolated KK modes.

Finally, the LD₅ geometry that is the essence of our model is also used in the weakly-interacting continuum proposal of [37]. However, here we do not identify dark matter as a population from an infinite, continuous set of weakly-coupled degrees of freedom, as proposed in [37].² Let us mention that a consistent way to realize such a picture is to

²The 4D degrees of freedom describing such a continuum become strongly-interacting in the bulk, since the strength of gravity grows with $r \rightarrow 0$ — notice that the EFT of gravity breaks down at sufficiently small r , see e.g. [38, 39]. Also, there is no well-defined narrow-width approximation for the 4D modes.

consider a weakly-coupled discretuum, as done in [40], whose properties are also reminiscent of the Dynamical Dark Matter framework of [41]. The phenomenology and nature of the dark matter in these discretized frameworks are very different from the holographic dark matter model presented here. In our model, dark matter instead arises from a strongly-coupled sector with no 4D weakly-coupled description.

1.2 Outline

This manuscript is organized as follows. Section 2 introduces the 5D dilaton-gravity background with a brane, and presents the properties of the associated holographic fluid. Section 3 focuses on a particular case of this background: the linear dilaton. We show that the holographic fluid constitutes a candidate for dark matter, and study its thermodynamics. Section 4 presents a natural freeze-in mechanism for holographic dark matter, that is computed both from the boundary and bulk perspectives. Section 5 presents phenomenological bounds on our model. Section 6 concludes, and App. A presents details on the linear dilaton graviton propagator and graviton emission.

2 Holographic Fluids

In this section we review a class of consistent solutions of the brane-dilaton-gravity system, that we refer to as the \mathcal{M}_ν spacetimes. We then review the low-energy 4D effective Einstein equation supported on the brane. In the presence of a bulk black hole, a perfect fluid naturally emerges in the effective Einstein equation, whose thermodynamics we study.

2.1 The \mathcal{M}_ν Spacetimes

We consider a 5D spacetime in the presence of a real scalar ϕ referred to as the *dilaton* field. The stabilization of the brane-gravity system often involves a flat *brane*. From the low-energy perspective, a brane is simply an infinitely thin hypersurface living in the higher dimensional spacetime and on which operators and degrees of freedom can be localized (see e.g. [42–44]).

We assume the bulk potential

$$V(\phi) = -\frac{3}{2}(4 - \nu^2)k^2 M_5^3 e^{2\nu\bar{\phi}}, \quad \bar{\phi} \equiv \phi/\sqrt{3M_5^3}, \quad (2.1)$$

where we introduced the 5D Planck scale M_5 . A fully consistent solution of the 5D Einstein field equations in the presence of this potential gives the metric [6]

$$ds^2 = g_{MN}dx^M dx^N = e^{-2A(r)}(-f(r)d\tau^2 + d\mathbf{x}^2) + \frac{e^{-2B(r)}}{f(r)}dr^2, \quad (2.2)$$

Instead, the infinite set of modes has a non-diagonal self-energy matrix, that mixes up all modes [39]. More generally, a nearly-free continuum is incompatible with standard gravity, see [2]. See also section 4.5.2 for a related consistency check in our model.

with

$$\begin{aligned} A(r) &= -\log(r/L), \\ B(r) &= -\nu^2 \log(r/r_b) + \log(\eta r), \quad \eta = k e^{\nu \bar{v}_b}, \\ f(r) &= 1 - \left(\frac{r_h}{r}\right)^{4-\nu^2}, \quad \bar{\phi}(r) = \bar{v}_b - \nu \log(r/r_b), \end{aligned} \quad (2.3)$$

with r_b the brane location, and v_b the value of the field ϕ at the brane as fixed by a brane-localized potential. The η parameter is a physical scale, and L is an integration constant with dimension of length that can be fixed to any value. The $f(r)$ function describes a planar black hole horizon located at $r = r_h \leq r_b$ in the bulk. See [5] for a careful treatment of the gauge redundancies and integration constants.

Finally, consistency arguments imply that the allowed range for ν is $0 \leq \nu < 2$ [6, 45]. The $\nu = 0$ case corresponds to the AdS_5 spacetime — with a bulk black hole and a brane.

2.2 Physics on the Brane: Einstein Equation and Holographic Fluids

The physics felt by a brane-localized observer is governed by the effective Einstein equation

$${}^{(4)}G_{\mu\nu} = \frac{1}{M_4^2} \left(T_{\mu\nu}^b + T_{\mu\nu}^{\text{eff}} \right) + O\left(\frac{T_b^2}{M_5^6}\right), \quad (2.4)$$

where $T_{\mu\nu}^b$ is the stress tensor of possible brane-localized matter. The 4D Planck mass is identified as $M_4^2 = M_5^3/\eta$. The indices in (2.4) are contracted with the induced metric on the brane, denoted by $\bar{g}_{\mu\nu}$. Equation (2.4) can be computed in a number of equivalent ways, see e.g. [45, 46].

We are assuming that all components of T_b are small compared to M_5 . In this low-energy limit, (2.4) takes the form of the standard Einstein equations with an extra effective stress tensor $T_{\mu\nu}^{\text{eff}}$. The structure of the $T_{\mu\nu}^{\text{eff}}$ tensor is identical to that of a 4-dimensional perfect fluid at rest,

$$T_{\nu}^{\text{eff},\mu} = g^{\mu\lambda} T_{\lambda\nu}^{\text{eff}} = \text{diag}(-\rho_{\text{eff}}, P_{\text{eff}}, \dots, P_{\text{eff}}), \quad (2.5)$$

that we refer to as the *holographic fluid*.

What are the properties of this holographic fluid? Let us choose the induced metric as

$$d\bar{s}^2 = -dt^2 + \left(\frac{r_b}{L}\right)^2 d\mathbf{x}^2, \quad (2.6)$$

where the 4D time t and the 5D time τ are related by $dt = e^{-A(r_b)} \sqrt{f(r_b)} d\tau$.

Tuning the brane tension to remove the effective 4D cosmological constant hidden in $T_{\mu\nu}^{\text{eff}}$, we can simply write $\rho_{\text{eff}} \equiv \rho_{\text{fluid}}$, $P_{\text{eff}} \equiv P_{\text{fluid}}$. Assuming that the horizon is very far

from the brane, i.e. $r_h \ll r_b$, we obtain the energy density and pressure

$$\rho_{\text{fluid}} = 3\eta^2 M_4^2 \left(\frac{r_h}{r_b} \right)^{4-\nu^2} \times \left[1 + \mathcal{O} \left(\frac{r_h^{4-\nu^2}}{r_b^{4-\nu^2}} \right) \right], \quad (2.7)$$

$$P_{\text{fluid}} = \eta^2 M_4^2 \left(\frac{r_h}{r_b} \right)^{4-\nu^2} \times \left[1 - \nu^2 + \mathcal{O} \left(\frac{r_h^{4-\nu^2}}{r_b^{4-\nu^2}} \right) \right]. \quad (2.8)$$

From these results we can infer the equation of state of the holographic fluid as $P_{\text{fluid}} = \omega_{\text{fluid}} \rho_{\text{fluid}}$. Focussing on the leading terms, we find that ω_{fluid} is constant with

$$w_{\text{fluid}} = \frac{1 - \nu^2}{3}. \quad (2.9)$$

Remarkably, since $0 \leq \nu < 2$, w_{fluid} interpolates between the values $\frac{1}{3}$ and -1 . This is precisely the range of values that has a familiar physical interpretation. For example, $\nu = 0$ corresponds to radiation behavior, while $\nu \rightarrow 2^-$ corresponds to vacuum energy behavior.

In short, the holographic fluid, at least at rest and for $r_h \ll r_b$, behaves just like a familiar perfect fluid, and its equation of state is controlled by the continuous parameter ν .

2.3 Thermodynamics of Holographic Fluids

We proceed with a brief analysis of the thermodynamics. We assume for the moment that the horizon is far from the brane, $r_h \ll r_b$.

The bulk black hole has a Hawking temperature. This temperature, upon appropriate redshifting, is perceived by a brane observer to be [6, 45]³

$$T_b = \frac{4 - \nu^2}{4\pi} \eta \left(\frac{r_h}{r_b} \right)^{1-\nu^2} \times \left[1 + \mathcal{O} \left(\frac{r_h^{4-\nu^2}}{r_b^{4-\nu^2}} \right) \right]. \quad (2.10)$$

This temperature is naturally interpreted as the holographic fluid temperature. The higher order corrections come from the effect of the blackening factor contained in the redshifting factor, $1/\sqrt{f(r_b)}$.

Similarly, the bulk black hole has an entropy density which, once redshifted to the brane observer, is given by

$$s_{\text{fluid}} = 4\pi\eta M_4^2 \left(\frac{r_h}{r_b} \right)^3 \times \left[1 + \mathcal{O} \left(\frac{r_h^{4-\nu^2}}{r_b^{4-\nu^2}} \right) \right]. \quad (2.11)$$

The free-energy density of the holographic fluid immediately follows:

$$f_{\text{fluid}} = \rho_{\text{fluid}} - T_b s_{\text{fluid}} = -\eta^2 M_4^2 \left(\frac{r_h}{r_b} \right)^{4-\nu^2} \times \left[1 - \nu^2 + \mathcal{O} \left(\frac{r_h^{4-\nu^2}}{r_b^{4-\nu^2}} \right) \right]. \quad (2.12)$$

³The temperature on the brane is obtained from the horizon temperature by multiplying with $1/\sqrt{|g_{\tau\tau}|}$.

Using this result, we can infer important information about the thermodynamical stability of the fluid. We can see that the free energy is negative (positive) for $\nu < 1$ ($\nu > 1$). This implies that the existence of the fluid, i.e. of the bulk black hole, is thermodynamically favored for $\nu < 1$ while it is unfavored for $\nu > 1$. Notice however that this conclusion assumes $r_h \ll r_b$. In the $\nu > 1$ case, it turns out that the presence of the fluid becomes favored at larger values of r_h [45].

Finally, for $\nu = 1$, the free energy vanishes at leading order. Therefore the next-to-leading order term must be determined to assess stability. This analysis is carried out in section 3.3.

3 Dark Matter as the $\nu = 1$ Holographic Fluid

In this section we interpret the \mathcal{M}_ν spacetime as a cosmological braneworld and identify the $\nu = 1$ holographic fluid as a dark matter candidate.

3.1 Braneworld Cosmology and Friedmann Equations

We assume that all the fields of the Standard Model are localized on the brane. The $T_{\mu\nu}^b$ stress tensor is identified as the SM stress tensor, $T_{\mu\nu}^b \equiv T_{\mu\nu}^{\text{SM}}$. The total stress tensor in the effective Einstein equation is thus $T_{\mu\nu}^{\text{tot}} = T_{\mu\nu}^{\text{SM}} + T_{\mu\nu}^{\text{fluid}}$.

We assume that the brane is moving, so that r_b depends on time. Within the low-energy regime assumed in (2.4), the brane motion is nonrelativistic and simplifications occur, see [1, 2] for details. The effective Einstein equation (2.4) then produces the effective Friedmann equations

$$3M_4^2 H^2 = \rho_{\text{tot}}, \quad 6M_4^2 \frac{\ddot{r}_b(t)}{r_b(t)} = -(\rho_{\text{tot}} + 3P_{\text{tot}}), \quad (3.1)$$

where $r_b(t)/L \equiv a(t)$ plays the role of the scale factor from the induced metric (2.6), with $H = \dot{r}_b/r_b$ the corresponding Hubble parameter. In these equations, we have $\rho_{\text{tot}} \simeq \rho_{\text{fluid}} + \rho_{\text{SM}}$, $P_{\text{tot}} \simeq P_{\text{fluid}} + P_{\text{SM}}$. The SM fields form a thermal bath with temperature T_{SM} , hence $\rho_{\text{SM}} = \rho_{\text{SM}}(T_{\text{SM}})$, $P_{\text{SM}} = P_{\text{SM}}(T_{\text{SM}})$.

The brane position today (i.e. at $t = t_0$) is denoted by $r_b(t_0) = r_{b,0}$.⁴ Assuming adiabatic expansion of the universe, we have $\frac{r_b(t)}{r_{b,0}} = \frac{T_{\text{SM},0}}{T_{\text{SM}}(t)}$, where $T_{\text{SM},0} = 0.23$ meV is the temperature of the universe today.

3.2 Dark Matter as a Holographic Fluid

In the \mathcal{M}_ν background with $\nu = 1$, the pressure of the holographic fluid vanishes up to $\mathcal{O}(r_h^3/r_b^3)$ corrections (see (2.8)). In the context of a cosmological braneworld model, we propose the identification [2, 5]

⁴One could assume $a(t_0) = 1$ without loss of generality, in which case $r_b(t_0) = L$. We do not make this assumption in the present work.

$$\text{Holographic fluid } (\nu = 1) \iff \text{Dark Matter}$$

In the following, we denote with the subscript DM all quantities related to the holographic fluid.

At leading order in the $\frac{r_h}{r_b}$ expansion, the thermodynamical properties of our dark matter candidate are

$$\rho_{\text{DM}}(t) = 3\eta^2 M_4^2 \left(\frac{r_h}{r_b(t)} \right)^3, \quad P_{\text{DM}} = 0, \quad f_{\text{DM}} = 0, \quad (3.2)$$

based on (2.7), (2.8), (2.10), (2.12). In terms of temperature, we have the scaling $\rho_{\text{DM}} = \rho_{\text{DM},0} \times \left(\frac{T_{\text{SM}}}{T_{\text{SM},0}} \right)^3$. Moreover, the DM temperature, i.e. the Hawking temperature as seen from a brane observer, is approximately constant, and is given by

$$T_{\text{DM}} \simeq \frac{3\eta}{4\pi}. \quad (3.3)$$

The corrections to this picture will be studied in section 3.3.

The constant temperature of DM is a hallmark of Hagedorn behavior. We remind that the above thermodynamical properties match those of the thermal state of Little String Theory [3, 4]. In LST, the Hagedorn temperature is identified as $T_H = \frac{M_s}{2\pi\sqrt{N}}$ [5], where M_s is the string scale.

Let us analyze the condition that guarantees that the holographic fluid accounts for the dark matter abundance today. Using today's critical density $\rho_{c,0} = 3H_0^2 M_4^2$, the DM abundance is given by the remarkably simple formula

$$\Omega_{\text{DM},0} = \left(\frac{\eta}{H_0} \right)^2 \left(\frac{r_h}{r_{b,0}} \right)^3. \quad (3.4)$$

Fixing the dark matter abundance to its observed value $\Omega_{\text{DM},0} \simeq 0.27$ relates therefore the ratio $r_h/r_{b,0}$ to the η parameter. Using today's value of the Hubble parameter $H_0 \simeq 1.47 \times 10^{-42}$ GeV, we obtain a bound on $\frac{r_h}{r_{b,0}}$. The bound can be extended to any time by considering the adiabatic expansion of the universe ($r_b \propto 1/T_{\text{SM}}$), from which we obtain

$$\frac{r_h}{r_b} \simeq 3.5 \times 10^{-16} \frac{T_{\text{SM}}}{\text{GeV}} \left(\frac{\text{GeV}}{\eta} \right)^{2/3}. \quad (3.5)$$

As a result, the horizon is typically very far from the brane, and the $\mathcal{O}(r_h^3/r_b^3)$ corrections are tiny, even for the maximum reheating temperature $T_{\text{SM},R}$ that we will find in section 4.

Since the \mathcal{M}_ν background has two physical parameters, our dark matter model has two parameters. Here we choose them to be $\{\eta, r_h\}$. Fixing the DM abundance relates these two parameters as given in (3.4). A mechanism for the formation of the black hole horizon, that determines r_h dynamically, will be presented in section 4.

3.3 Holographic Dark Matter Thermodynamics

In this subsection we perform a more precise analysis of the thermodynamics of the holographic fluid identified as dark matter.

The first law of thermodynamics dictates that the variation of the total energy of a closed system satisfies $dU = TdS - PdV$ where U and S are extensive quantities. In particular, for the holographic fluid at temperature T_{DM} we have

$$dU(r_h, r_b) = T_{\text{DM}} dS(r_h, r_b) - P(r_h, r_b) dV(r_b), \quad (3.6)$$

which implies

$$\left[\frac{\partial U}{\partial r_h} - T_{\text{DM}} \frac{\partial S}{\partial r_h} \right] dr_h + \left[\frac{\partial U}{\partial r_b} + P \frac{\partial V_b}{\partial r_b} - T_{\text{DM}} \frac{\partial S}{\partial r_b} \right] dr_b = 0. \quad (3.7)$$

The exact temperature is

$$T_{\text{DM}}(x_h) = \frac{T_H}{f_b^{1/2}}, \quad T_H \equiv \frac{3\eta}{4\pi}, \quad (3.8)$$

where T_H is the Hagedorn temperature, and the blackening factor is $f_b(x_h) = 1 - x_h^3$, where we introduced the $x_h = r_h/r_b$ variable. The T_{DM} temperature differs from T_H by a $\mathcal{O}(x_h^3)$ correction, which was neglected in the previous sections. We have $T_{\text{DM}} \geq T_H$.

We also know the exact free energy density f_{DM} , which is the on-shell action (see e.g. [45]). Using the free energy and temperature, and combining with the thermodynamical relations (3.7), we are able to derive the entropy and energy density. The results are

$$\frac{\rho_{\text{DM}}}{\eta^2 M_4^2} = 6 \left(1 - f_b^{1/2} \right), \quad (3.9)$$

$$\frac{s_{\text{DM}}}{\eta M_4^2} = 4\pi (1 - f_b), \quad (3.10)$$

$$\frac{f_{\text{DM}}}{\eta^2 M_4^2} = \frac{\rho_{\text{DM}} - T_{\text{DM}} s_{\text{DM}}}{\eta^2 M_4^2} = -\frac{3}{f_b^{1/2}} \left(1 - f_b^{1/2} \right)^2. \quad (3.11)$$

Expanding these formulas for $x_h \ll 1$ reproduces the values in (3.2). In particular, the free energy density vanishes up to $\mathcal{O}(x_h^3)$ corrections, such that $f_{\text{DM}} = \mathcal{O}(x_h^3)$. From this we can see that $f_{\text{DM}} < 0$ for any value of $r_h > 0$. This implies that for $T_{\text{DM}} > T_H$ the black hole phase is always favored with respect to the no-black hole phase.⁵ This result is consistent with the analysis of LST done in [47].

We can write (3.10)-(3.11) in terms of T_{DM} using that

$$f_b(T_{\text{DM}}) = \left(\frac{T_H}{T_{\text{DM}}} \right)^2, \quad (3.12)$$

⁵The situation is different for $\nu > 1$, in which case the black hole phase is energetically favored only for r_h above a finite value, see [45].

which gives

$$\frac{s_{\text{DM}}}{\eta M_4^2} = 4\pi \left(1 - \frac{T_H^2}{T_{\text{DM}}^2}\right), \quad \frac{\rho_{\text{DM}}}{\eta^2 M_4^2} = 6 \left(1 - \frac{T_H}{T_{\text{DM}}}\right), \quad \frac{f_{\text{DM}}}{\eta^2 M_4^2} = -3 \frac{(T_{\text{DM}} - T_H)^2}{T_{\text{DM}} T_H}. \quad (3.13)$$

These expressions are valid for $T_{\text{DM}} \geq T_H$, with T_{DM} being typically very close to T_H . We can notice the important feature that $f_{\text{DM}}(T_{\text{DM}})$ and $f'_{\text{DM}}(T_{\text{DM}})$ vanish at $T_{\text{DM}} = T_H$ while $f''_{\text{DM}}(T_{\text{DM}})$ does not.

Using these results, it is possible to study the behavior of our thermodynamical system in terms of the brane temperature, $T_{\text{DM}} = T_{\text{DM}}(T_{\text{SM}})$. Using Eq. (3.8) and the adiabatic expansion of the universe, we have

$$T_{\text{DM}}(T_{\text{SM}}) = \frac{T_H}{\sqrt{1 - \left(\frac{r_h}{r_{b,0}}\right)^3 \left(\frac{T_{\text{SM}}}{T_{\text{SM},0}}\right)^3}}. \quad (3.14)$$

Notice that the idea of using thermodynamical variables defined on the boundary of the system has been long known, see [48, 49]. The general principle of our analysis is analogous, except that here the black hole is not in thermal equilibrium with the brane.

The free energy of the black hole phase is given by (3.13) taken as a function of T_{DM} , $f_{\text{DM}} = f_{\text{DM}}(T_{\text{DM}})$. The free energy of the phase with no black hole is $f_{\text{no BH}}(T_{\text{SM}}) = 0$ for all $T_{\text{SM}} \geq 0$. Using (3.13), we find that $f_{\text{DM}}(T_H) = f'_{\text{DM}}(T_H) = 0$, which implies that there is a continuous phase transition at $T_{\text{DM}} = T_H$. The phase transition being continuous, no supercooling is possible, and we conclude that the system is in the black hole phase for any $T_{\text{DM}} > T_H$. This applies in particular to the cosmological braneworld model.

Finally we can also compute the DM speed of sound, defined by $c_{\text{DM}}^2 \equiv -\frac{\partial f_{\text{DM}}}{\partial \rho_{\text{DM}}} = -\frac{f'_{\text{DM}}(x_h)}{\rho'_{\text{DM}}(x_h)}$, as

$$c_{\text{DM}}^2 = \frac{1}{2} \frac{x_h^3}{1 - x_h^3} = \frac{1}{2T_H^2} (T_{\text{DM}}^2 - T_H^2). \quad (3.15)$$

In the present work, x_h is extremely small, i.e. $r_h \ll r_b$, c.f. (3.5), so that $c_{\text{DM}}^2 \ll 1$.

One may notice that, when the black hole comes very close to the brane, (3.15) would give $c_{\text{DM}} > 1$, which is forbidden. This occurs for $T_{\text{DM}} > \sqrt{3} T_H$, which corresponds to $r_b \lesssim 1.14 r_h$. This problem seems to be related to the ambiguity in the definition of the BH vacuum state, as it was argued in Ref. [13] (see also Ref. [50]). This extreme regime is not relevant for our study.

Brief summary. Our thermodynamical analysis of the $\nu = 1$ holographic fluid establishes that

- The system is always in the black hole phase for any $T_{\text{SM}} > 0$.
- The DM sound speed is nonzero but small, with typically $c_{\text{DM}}^2 \sim \frac{x_h^3}{2}$.

3.4 On the Model Parameters

Let us discuss the free parameters of the model. The $\mathcal{M}_{\nu=1}$ background has two free parameters, that can be chosen to be $\{\eta, r_h\}$. The other parameters $\{M_5, T_{\text{DM}}\}$ appearing in the model satisfy the relations

$$M_5^3 = \eta M_4^2, \quad T_{\text{DM}} = \frac{3\eta}{4\pi} \frac{1}{\sqrt{1 - (r_h/r_b)^3}}. \quad (3.16)$$

We remind that M_4 is the 4D Planck mass. If one neglects r_h/r_b , then T_{DM} is simply proportional to η . If the mild dependence in r_h is taken into account, T_{DM} becomes an independent parameter that could be traded for r_h , although such a choice would be unpractical since it would involve a fine cancelation between T_{DM} and $T_H = \frac{3\eta}{4\pi}$.

One combination of our two free parameters is fixed by the value of DM abundance today obtained from (3.4). Our model has thus a single free parameter. In the following we choose that r_h is fixed by the DM abundance, while η (or equivalently M_5) remains as the free parameter. The phenomenological bounds on the free parameter are presented in section 5. In the next section a dynamical mechanism for DM formation is presented, that does not change the parameter counting.

4 Freeze-in Production of Holographic Dark Matter

Having identified the $\nu = 1$ holographic fluid as the cosmological dark matter observed in our universe, we should ask about the cosmological history of such a scenario. Is there a mechanism capable of producing the holographic fluid with correct abundance in the early universe?

In this section we show that a mechanism analogous to freeze-in production [51] naturally occurs in our holographic dark matter framework. This is the mechanism sketched in section 1. The freeze-in computation will be done from both the brane and bulk perspectives. Even though the intermediate steps appear different, the final results perfectly match, thereby demonstrating the self-consistency of the whole formalism.

Our main assumption is that the inflaton is brane-localized. As a result, the brane position r_b (i.e. the scale factor) grows exponentially during inflation, such that the bulk can be considered as empty at the end of inflation. It is thus well-motivated to consider the system at the reheating time with no bulk black hole, i.e. $r_h = 0$. The corresponding reheating temperature is denoted $T_{\text{SM},R}$.

4.1 Heating the Bulk: Graviton Radiation from the Brane

The Standard Model particles on the brane couple to bulk gravitons as

$$\mathcal{L} \supset -\frac{1}{M_5^{3/2}} T_{\text{SM}}^{\mu\nu}(x) h_{\mu\nu}(z_b, x). \quad (4.1)$$

Therefore, processes of the form $\varphi + \bar{\varphi} \rightarrow h_{\mu\nu}$ happen in the brane thermal bath. Since the gravitons live in the bulk, this is an emission mechanism through which energy is transferred from the brane to the bulk.

The rate of this energy transfer process, here denoted $\Delta\dot{\rho}_{\text{SM}}$, was estimated in [9] and computed in AdS_5 in [13–15]. We perform a computation of $\Delta\dot{\rho}_{\text{SM}}$ in the LD_5 background using a unitarity cut on the LD propagators computed in [5, 6]. The details of the computation are given in App. A. For center-of-mass energy much higher than the local 5D curvature $R|_{\text{brane}} \approx -12\eta^2$, the result matches the flat space result (as well as the AdS_5 with negligible curvature, as done in [13–15]).

The brane-to-bulk energy transfer rate is

$$\Delta\dot{\rho}_{\text{SM}} = -\frac{2\left(\sum_{\varphi} g_{\varphi} \kappa_{\varphi}^2 c_{\varphi} a_{\varphi}\right)}{5\pi^4 \eta M_4^2} \Gamma\left(\frac{7}{2}\right) \Gamma\left(\frac{9}{2}\right) \zeta\left(\frac{7}{2}\right) \zeta\left(\frac{9}{2}\right) T_{\text{SM}}^8, \quad (4.2)$$

where $a_s = a_V = 1$, $a_f \simeq 0.75$ (s , V and f stand for scalars, vectors and fermions, respectively), and c_{φ} is given by Eq. (A.18). Considering the SM degrees of freedom with $g_s = 4$, $g_V = 12$ and $g_f = 45$ we get $\sum_{\varphi} g_{\varphi} \kappa_{\varphi}^2 c_{\varphi} a_{\varphi} = 20.78$, where κ_{φ} is the number of spin degrees of freedom of φ ($\kappa_s = 1$ and $\kappa_V = \kappa_f = 2$). Numerically,

$$\Delta\dot{\rho}_{\text{SM}} = -C_{\rho} \frac{T_{\text{SM}}^8}{\eta M_4^2}, \quad C_{\rho} \simeq 3.919. \quad (4.3)$$

4.2 Evolution Equations: Boundary Viewpoint

The 4D effective Einstein equation (2.4) leads to a 4D effective conservation equation. It can be derived either by contracting with ∇^{μ} and using the 4D Bianchi equation, or by starting with the 5D conservation equation and projecting it on the brane, see [1, 2] for details and checks. The effective conservation equations for the SM and DM energy densities are

$$\dot{\rho}_{\text{SM}} = -4H\rho_{\text{SM}} + \Delta\dot{\rho}_{\text{SM}}, \quad (4.4)$$

$$\dot{\rho}_{\text{DM}} = -3H\rho_{\text{DM}} + \Delta\dot{\rho}_{\text{DM}}, \quad \Delta\dot{\rho}_{\text{SM}} + \Delta\dot{\rho}_{\text{DM}} = 0. \quad (4.5)$$

Since by definition $\rho_{\text{DM}} \propto r_h^3$ (see (3.2)), the evolution equation (4.5) can alternatively be thought as an evolution equation for the r_h parameter. That is, the equation must describe the evolution of the black hole horizon in the bulk, providing a geometric picture of freeze-in. The evolution equation for r_h is found to be

$$9M_4^2 \eta^2 \frac{\dot{r}_h r_h^2}{r_b^3} = \Delta\dot{\rho}_{\text{DM}}. \quad (4.6)$$

In next section we show that this result can be derived directly from the bulk viewpoint.

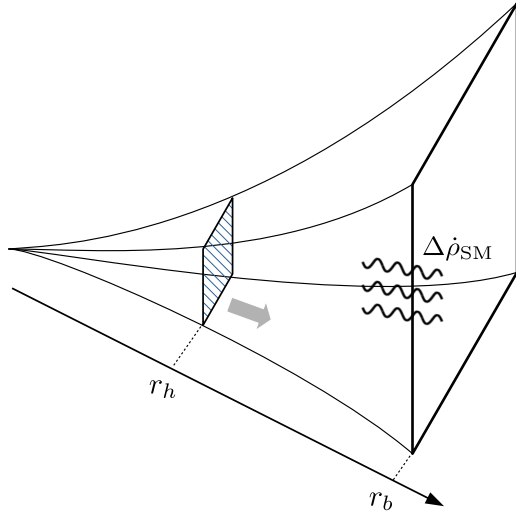


Figure 1. The freeze-in of holographic dark matter.

4.3 Evolution Equations: Bulk Viewpoint

The radiation can be modeled using a Vaidya-like metric [52, 53], which describes the spacetime surrounding a radiating relativistic star. The underlying approximation is that the radiation is emitted orthogonally to the brane [15]. This approximation holds when the brane is non-relativistic and therefore applies in the low-energy regime that is our working assumption.

Along the same lines, we assume that the brane motion is negligible compared to the motion of the bulk horizon, i.e. $\dot{r}_h \gg \dot{r}_b$. That is, we assume that the freeze-in timescale is much smaller than the universe's expansion. The validity of these assumptions will be verified a posteriori. The geometry is summarized in Fig. 1.

We introduce the light-like coordinate v

$$v = t + \int \frac{dr}{f(r)} \frac{L}{r\eta rr_b}, \quad (4.7)$$

for which the metric takes the form

$$ds^2 = -f(v, r) \frac{r^2}{L^2} dv^2 + 2 \frac{r}{L \eta r_b} dv dr + \frac{r^2}{L^2} dx^2. \quad (4.8)$$

In the static limit for which r_h is constant, i.e. the f factor only depends on r , one can verify that (4.8) is equivalent to the original linear dilaton metric (2.1).

Using this metric, radiation is described by the bulk stress-energy tensor

$${}^{(5)}T_{MN}^{\text{rad}} \equiv \Delta \dot{\rho}_{\text{DM}} k_M k_N, \quad (4.9)$$

where $\Delta\dot{\rho}_{\text{DM}} = \frac{d}{dt}\Delta\rho_{\text{SM}}$ is the energy transfer rate in the brane time, and k_M is a null vector.

k_M is chosen to satisfy $k_M u^M = 1$, with u^M the timelike unit velocity vector for brane observers, $u^M = (\dot{v}, \dot{r}, \mathbf{0})$. Using the metric (4.8), the only non-vanishing component of k_M is k_t (or k^r). Moreover, $k_M u^M = 1$ implies $k_t = 1/\dot{v}$. Finally, the normalization $u^M u_M = -1$ gives

$$\dot{v} \approx \frac{L}{r\sqrt{f(v, r)}}, \quad (4.10)$$

where we used the nonrelativistic limit for which \dot{r} can be neglected.⁶

Turning to the Einstein tensor, we find that only the vv component depends on the variation of r_h , $\frac{d}{dv}r_h$. The vv component of the Einstein equation, $M_5^3 {}^{(5)}G_{vv} = {}^{(5)}T_{vv}^{\text{rad}}$, implies

$$9LM_4^2\eta^2r_b r_h^2 \frac{d}{dv}r_h = 2\Delta\dot{\rho}_{\text{DM}}r^5f. \quad (4.12)$$

We evaluate (4.12) on the brane, set $r = r_b$, $f \approx 1$, and use $\frac{d}{dv} = \frac{d}{\dot{v}dt}$. Notice that the L dependence vanishes. The result gives precisely the evolution equation (4.6) — up to a factor 2 coming from the fact that in the above description, the brane radiates on both sides, as noticed in [14].

4.4 Initial Condition

We assume that our holographic model is valid during inflation. We further assume that the inflaton field is brane-localized. Geometrically, this implies that $\dot{r}_b \propto e^{Ht}$, i.e. the brane runs away exponentially towards positive r . As a result of the braneworld inflation, we have $r_h \sim 0$, i.e. the holographic fluid is nonexistent at the end of inflation. In this section we call $r_h(T)$ the value of the horizon as a function of the temperature, as given by sections 4.3 and 4.2, while its constant value at small temperatures (i.e. in standard cosmology) will be denoted as \bar{r}_h .

In this work we do not specify the inflation mechanism, and simply start at the reheating time, with corresponding temperature $T_{\text{SM},R}$.⁷ The initial condition for the dark matter energy density is

$$\rho_{\text{DM}}(T_{\text{SM},R}) = 0. \quad (4.13)$$

4.5 Holographic Dark Matter Freeze-In

In this subsection we solve the evolution equations (4.4) and (4.5). Let us first notice that, for low temperatures, the energy transfer term $\Delta\dot{\rho}_{\text{SM,DM}}$ is negligible as compared to the other terms in the conservation equations. Because of the initial condition (4.13), we can also assume that $\rho_{\text{SM}} \gg \rho_{\text{DM}}$ throughout the evolution of the Universe, such that the Hubble parameter is controlled by the SM thermal bath,

$$H = \frac{1}{\sqrt{3}M_4} \sqrt{\rho_{\text{SM}} + \rho_{\text{DM}}} \simeq \frac{1}{\sqrt{3}M_4} \sqrt{\rho_{\text{SM}}}. \quad (4.14)$$

⁶The exact relation is

$$\dot{v} = \frac{L}{\eta r_b f r} \left(\dot{r} + \sqrt{\dot{r}^2 + \eta^2 r_b^2 f} \right). \quad (4.11)$$

⁷Notice however that the scenario is well-motivated by e.g. the trace anomaly driven inflation mechanism of [54].

These points imply that, at low temperatures, the scaling of ρ_{SM} and ρ_{DM} from standard cosmology is recovered. We denote the corresponding quantities in standard cosmology with bars,

$$\bar{\rho}_{\text{SM}}(T_{\text{SM}}) \propto T_{\text{SM}}^4, \quad \bar{\rho}_{\text{DM}}(T_{\text{SM}}) \propto T_{\text{SM}}^3. \quad (4.15)$$

Furthermore, we have that $|\Delta\dot{\rho}_{\text{SM},R}| \ll H\rho_{\text{SM}}(T_{\text{SM},R})$ at reheating. Therefore the correction to the SM energy density is small, and we can write

$$\rho_{\text{SM}}(T_{\text{SM}}) \approx \bar{\rho}_{\text{SM}}(T_{\text{SM}}) = g_* \frac{\pi^2}{30} T_{\text{SM}}^4 \quad (4.16)$$

to a very good approximation.

Using these simplifications, we now solve the evolution equation (4.5). The result is

$$\rho_{\text{DM}}(T_{\text{SM}}) = \frac{\sqrt{10}C_\rho}{\pi\eta M_4\sqrt{g_*}} T_{\text{SM}}^3 (T_{\text{SM},R}^3 - T_{\text{SM}}^3) \quad (4.17)$$

$$= \bar{\rho}_{\text{DM}}(T_{\text{SM}}) \times \left(1 - \frac{T_{\text{SM}}^3}{T_{\text{SM},R}^3}\right), \quad (4.18)$$

with

$$\bar{\rho}_{\text{DM}}(T_{\text{SM}}) = \frac{\sqrt{10}C_\rho}{\pi\eta M_4\sqrt{g_*}} T_{\text{SM},R}^3 T_{\text{SM}}^3. \quad (4.19)$$

This result constitutes the prediction for the dark matter energy density in our holographic model. From (4.18), we can see that the freeze-in production occurs within roughly one order of magnitude in temperature below $T_{\text{SM},R}$.

The freeze-in production of the dark fluid can equivalently be interpreted as the freeze-in production of the black hole horizon, as given by (4.6) and (4.12), with solution

$$r_h^3(T_{\text{SM}}) = \bar{r}_h^3 \left(1 - \frac{T_{\text{SM}}^3}{T_{\text{SM},R}^3}\right), \quad \bar{r}_h^3 = \frac{\sqrt{10}C_\rho}{3\pi\sqrt{g_*}} \left(\frac{LT_{\text{SM},0}}{\eta M_4}\right)^3 T_{\text{SM},R}^3, \quad (4.20)$$

from where we can see that $\bar{r}_h = r_h(T_{\text{SM}} \ll T_{\text{SM},R})$. Then (3.2) can be written as

$$\rho_{\text{DM}}(T_{\text{SM}}) = 3\eta^2 M_4^2 \left(\frac{r_h(T_{\text{SM}})}{r_b(T_{\text{SM}})}\right)^3. \quad (4.21)$$

Identifying with (3.4), the dark matter abundance predicted by freeze-in is found to be

$$\Omega_{\text{DM},0} = \frac{\sqrt{10}C_\rho}{3\pi\sqrt{g_*}\eta H_0^2} \left(\frac{T_{\text{SM},R} T_{\text{SM},0}}{M_4}\right)^3. \quad (4.22)$$

Finally, the energy-to-entropy density ratio is given by

$$\frac{\rho_{\text{DM}}}{s_{\text{tot}}} = \frac{45\sqrt{10}C_\rho g_{*,S}}{2\pi^3\sqrt{g_*}} \frac{T_{\text{SM},R}^3 - T_{\text{SM}}^3}{\eta M_4}, \quad (4.23)$$

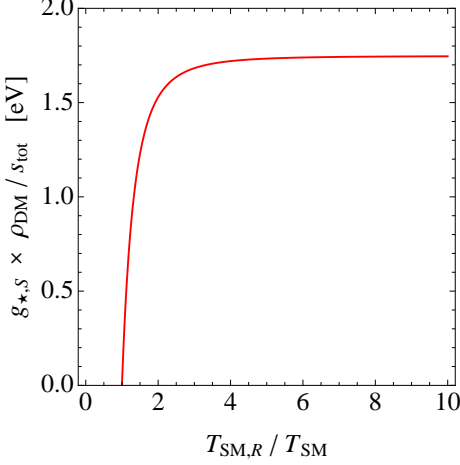


Figure 2. Energy-to-entropy ratio $\rho_{\text{DM}}/s_{\text{tot}}$, normalized by $g_{*,S}$, as a function of $T_{\text{SM},R}/T_{\text{SM}}$. This quantity freezes at temperature $T_{\text{SM}} \ll T_{\text{SM},R}$.

where we used $s_{\text{tot}} \approx s_{\text{SM}} = g_{*,S} \frac{2\pi^2}{45} T_{\text{SM}}^3$ and $g_{*,S}$ is the entropy effective number of degrees of freedom in the SM. This result is shown in Fig. 2.

4.5.1 Discussion

From (4.22), we relate the reheating temperature to the model parameters. Keeping M_5 as the free parameter, we find

$$T_{\text{SM},R} = \left[\frac{3\pi\Omega_{\text{DM},0}\sqrt{g_*}}{C_\rho\sqrt{10}} \eta H_0^2 \right]^{1/3} \frac{M_4}{T_{\text{SM},0}} \simeq 9.4 \times 10^{-10} M_5. \quad (4.24)$$

Moreover, considering the bound $M_5 \lesssim M_4$ (which corresponds to $\eta \lesssim M_4$) yields for the reheating temperature the upper bound

$$T_{\text{SM},R} \lesssim 2.3 \times 10^9 \text{ GeV}. \quad (4.25)$$

This is in good agreement with most realistic inflationary models [55].

Finally, the value of the reheating temperature $T_{\text{SM},R}$ in (4.24) needs to satisfy the consistency requirement $\rho_{\text{SM}}(T_{\text{SM},R}) \lesssim \eta^2 M_4^2$, ensuring the validity of the low-energy approximation used in the effective Einstein equation (2.4). This translates into the mild (sufficient) condition $M_5 \gtrsim 10 \text{ GeV}$, valid for $T_{\text{SM}} < T_{\text{SM},R}$.

As expected for freeze-in production, the DM sector is never in thermal equilibrium with the SM as condition (4.24) guarantees that $\rho_{\text{DM}} \ll \rho_{\text{SM}}$ at temperatures $T_{\text{SM}} \leq T_{\text{SM},R}$ (radiation domination). This also justifies one of the assumptions done in the solving of the evolution equations. The remaining assumption, that $|\Delta\dot{\rho}_{\text{SM}}| \ll H\rho_{\text{SM}}$ for any $T_{\text{SM}} \leq T_{\text{SM},R}$, is verified explicitly by using the relation (4.24) in the explicit expression for $\Delta\dot{\rho}_{\text{DM}}$ given in (4.3).

4.5.2 Emitted gravitons versus dark matter density

It is possible to compute the total number of emitted gravitons using the Boltzmann equation on the brane. The result is $n_{\text{emitted}} \propto \frac{T_{\text{SM},R}^2 T_{\text{SM}}^3}{\eta M_4}$. On the other hand, the energy density of holographic dark matter obtained in (4.19) behaves as $\rho_{\text{DM}} \propto \frac{T_{\text{SM},R}^3 T_{\text{SM}}^3}{\eta M_4}$. For non-relativistic matter, one would expect that the ratio of these expressions corresponds to a physical mass scale, i.e. $\frac{\rho}{n} \approx m$. Here, instead, we find that the ratio is proportional to $T_{\text{SM},R}$, and thus depends on the initial condition. This discrepancy illustrates the fact that n_{emitted} should not be identified as some dark matter number density. Notice that, from the 4D dual perspective, a strongly-coupled theory generally does not have particle states. Thus the notion of number density does not even exist — the physical quantities relevant for gravity are energy and pressure.

5 Phenomenological Constraints

In this section we collect cosmological, astrophysical and laboratory bounds which constrain the holographic dark matter model. The model has a single free parameter, see discussion in section in 3.4. Here we express the bounds in terms of the 5D Planck scale M_5 .

5.1 Dark Matter Sound Speed

In section 4 we have determined the speed of sound of holographic dark matter, (3.15). This sound speed depends on $r_h^3/r_{b,0}^3$, which is related to M_5 by imposing the observed DM energy density,

$$\frac{r_h}{r_{b,0}} \simeq 2.7 \times 10^{-4} \left(\frac{\text{GeV}}{M_5} \right)^2 \quad (5.1)$$

as shown in (3.5). The dark matter sound speed is constrained using galactic rotation curves [56] as

$$c_{\text{DM}} \lesssim 10^{-4}. \quad (5.2)$$

Combining (3.15) and (5.1), this bound translates as a mild bound on M_5 ,

$$M_5 \gtrsim 300 \text{ MeV}. \quad (5.3)$$

5.2 Supernovae Cooling

The bulk gravitons can be produced in supernovae (SN) [57, 58]. If the energy loss due to graviton emission into the bulk were excessive, it would change stellar evolution [59]. Numerical studies of SN energy losses reveal that the neutrino burst would have been excessively shortened unless the energy loss rate of the SN core obeys

$$Q_{\text{SN}} \lesssim 3 \times 10^{33} \text{ erg cm}^{-3}\text{s}^{-1} \simeq 10^{-29} \text{ GeV}^5. \quad (5.4)$$

This corresponds to the strongest constraint based on the analysis of SN1987A.

Assuming a SN temperature of $T_{\text{SN}} = 30 \text{ MeV}$, the SN energy loss rate is directly given by the graviton emission rate $\Delta\dot{\rho}_{\text{SM}}$ computed in (4.3), with

$$Q_{\text{SN}} = \Delta\dot{\rho}_{\text{DM}} = C_\rho \frac{T_{\text{SN}}^8}{M_5^3}. \quad (5.5)$$

Combining with the bound (5.4), we obtain the constraint

$$M_5 \gtrsim 648 \text{ TeV}. \quad (5.6)$$

Here we have assumed that the graviton mass gap is negligible with respect to $\eta \ll T_{\text{SN}}$, which is verified a posteriori from the value (5.6).

This bound is stronger than the bounds in [58] on unparticles coupled to photons or electrons, as here the graviton continuum is coupled to all SM particles through their energy-momentum tensor.

5.3 Big Bang Nucleosynthesis (BBN)

In section 4 we have shown that the freeze-in mechanism, upon imposing the observed DM energy density, implies a relation between the reheating temperature $T_{\text{SM},R}$ and M_5 given by (4.24). To avoid disturbing the mechanism of BBN, the reheating temperature must satisfy the lower bound $T_{\text{SM},R} \gtrsim 4 \text{ MeV}$. This translates into a bound on M_5 as

$$M_5 \gtrsim 4.3 \times 10^3 \text{ TeV}. \quad (5.7)$$

5.4 Deviation to Newtonian Potential

The Newtonian potential at present times in a braneworld model can be deduced from the graviton brane-to-brane propagator [2]. In the linear dilaton braneworld of our focus, the Newton potential for two particles of masses m_1 and m_2 at a distance R is given by

$$V_N(R) = -G_N \frac{m_1 m_2}{R} [1 + \Delta(R)], \quad (5.8)$$

where

$$\Delta(R) \simeq \begin{cases} \frac{8}{9\pi\eta R} & \text{if } \eta R \lesssim 1 \\ \frac{8}{9\sqrt{3}\pi} \frac{1}{(\eta R)^{3/2}} e^{-\frac{3}{2}\eta R} & \text{if } \eta R \gtrsim 1 \end{cases}. \quad (5.9)$$

Torsion pendulum (fifth-force) experiments [60–62] constrain deviations to gravity down to the micrometer scale. In the context of our linear dilaton braneworld, we use the bound $\Delta(R) \lesssim 10^{-2}$ at $R \sim 50 \mu\text{m}$.⁸ Applying this bound to (5.9) at $R \sim 1/\eta$ provides the constraint $\eta \gtrsim 6 \text{ meV}$. Translating to M_5 we obtain

$$M_5 \gtrsim 3 \times 10^5 \text{ TeV}. \quad (5.10)$$

⁸Beyond gravity, the $\propto \frac{1}{r^2}$ fifth force can also be induced by coupling to a CFT operator with conformal dimension 3/2 [63, 64].

5.5 Discussion

The strongest phenomenological bound on the 5D Planck mass, $M_5 \gtrsim 3 \times 10^5$ TeV, comes from the correction to the Newtonian potential.

The lower bounds on M_5 translate as lower bounds on the reheating temperature through (4.24). From the fifth force bound of (5.10), we obtain the mild bound $T_{\text{SM},R} \gtrsim 300$ MeV. The lowest value allowed is a fairly low reheating temperature, but still consistent with the Standard Cosmological Model [65].

Since the graviton couples to the SM with strength $M_5^{-3/2}$, the above bounds from the fifth force, supernovae, and BBN are all typically stronger than those achievable from present (LHC) or future (FCC-hh) colliders [66, 67]. In fact, the partonic cross-section production at colliders goes like $\hat{\sigma} \sim \sqrt{\hat{s}}/M_5^3$, where $\sqrt{\hat{s}}$ is the partonic center-of-mass energy. Typically, we can consider for FCC-hh $\sqrt{\hat{s}} < 100$ TeV, which provides, using the bound (5.10), a production cross-section $\hat{\sigma} \lesssim 10^{-9}$ fb. For integrated luminosities as high as 10^5 fb $^{-1}$ the signal would be below the observability limit.

At the level of laboratory experiments, future probes of the Newtonian potential, such as optically-levitated sensors [68] probing sub- μm distances, are likely more promising to further constrain the M_5 parameter.

6 Summary and Outlook

What is dark matter made of? In this work we have developed the idea that dark matter is a fluid/plasma formed in a hidden, strongly-coupled sector. Building on our previous works [1, 2], we provide a holographic description of the DM fluid in terms of the 5D linear dilaton braneworld. From the 5D viewpoint, the fluid on the brane originates from a planar black hole in the bulk.

We have studied in detail the thermodynamic properties of the holographic fluid, going beyond the far-horizon approximation $r_h \ll r_b$. In this limit, the fluid exhibits Hagedorn thermodynamics, hence the free energy vanishes. Going beyond this approximation is essential to determine the properties of the black hole phase. We find that the black hole phase is thermodynamically preferred for all radii, and that the associated phase transition is continuous. As a consequence, the cosmological braneworld is always in the black hole phase, as required for the holographic description of DM. We also find that the equation of state receives small corrections, and that the dark matter sound speed is very small but nonzero.

We then present a natural freeze-in mechanism for the emergence of DM in the early universe, relying solely on the assumption that the inflaton is brane-localized. Under this assumption, the bulk is effectively empty at the time of reheating. After reheating, gravitons are emitted from the brane into the bulk. The energy transferred from the SM thermal bath into the bulk through this process triggers the smooth formation of a horizon. This freeze-in formation of the bulk black hole lasts over one order of magnitude in temperature, after which the horizon remains unchanged.

Technically, we present the freeze-in calculation from both the boundary and bulk perspectives, and show that the two descriptions are equivalent. The boundary calculation relies on the effective four-dimensional conservation equation. The bulk calculation models the emitted gravitons using a Vaidya-type metric, with the evolution of the horizon following directly from solving the 5D Einstein equations.

After fixing the dark matter abundance to its observed value, the model features a single free parameter. We choose this parameter to be the 5D Planck mass M_5 . We find that the model is constrained by BBN through the reheating temperature and by supernovae due to bulk graviton emission, with $M_5 > \mathcal{O}(10^3)$ TeV. These bounds are dwarfed by torsion pendulum experiments that give $M_5 > \mathcal{O}(10^5)$ TeV as leading constraint. A constraint on the DM sound speed also places a modest $\mathcal{O}(\text{GeV})$ bound on M_5 .

Given these constraints, probing the graviton continuum at present or future colliders does not appear feasible. More promising prospects may instead come from future probes of the Newtonian potential, such as optically-levitated sensors [68], which could test the graviton continuum at sub- μm distances.

Finally, our model has been used so far to describe the homogeneous dark matter distribution. More evolved spherical halo solutions are required to describe the heterogeneous universe. Our search for $O(3)$ -symmetric solutions is in progress, see [69] for an encouraging related result.

Acknowledgments

EM would like to thank the ICTP South American Institute for Fundamental Research (SAIFR), São Paulo, Brazil, for hospitality and partial financial support during the final stages of this work. The work of EM is supported by the “Proyectos de Investigación Pre-competitivos” Program of the Plan Propio de Investigación of the University of Granada under grant PP2025PP-18. The work of MQ is supported by the grant PID2023-146686NB-C31 funded by MICIU/AEI/10.13039/501100011033/ and by FEDER, EU. IFAE is partially funded by the CERCA program of the Generalitat de Catalunya. SF is supported by grant 2021/10128-0 of FAPESP.

A Computing Graviton Radiation from the Brane

We present the calculation of the graviton emission rate from the brane used in section 4.1.

A.1 Graviton Propagator

The graviton field is the tensor fluctuation of the 5D metric. For our purposes it is sufficient to focus on the transverse traceless component $\tilde{h}_{\mu\nu}$, normalized as

$$ds^2 = e^{-2A(z)} \left[\left(\eta_{\mu\nu} + \frac{2}{M_5^{3/2}} \tilde{h}_{\mu\nu}(x, z) \right) dx^\mu dx^\nu + dz^2 \right], \quad (\text{A.1})$$

where we are using conformal coordinates.⁹ In these coordinates, the brane at $z = z_b$ partitions the space \mathcal{M} into two subspaces $\mathcal{M}^- \equiv \mathcal{M}|_{[z_b, \infty)}$, $\mathcal{M}^+ \equiv \mathcal{M}|_{(-\infty, z_b]}$.

We find it convenient to work with the rescaled field $h_{\mu\nu}(x, z)$ defined by

$$h_{\mu\nu}(x, z) = e^{-3A(z)/2} \tilde{h}_{\mu\nu}(x, z), \quad (\text{A.2})$$

whose normalization in the extra dimension is computed as $\|\tilde{h}\|^2 \equiv \int dz |\tilde{h}_{\mu\nu}(x, z)|^2$. The corresponding 5D graviton propagator in spacetime \mathcal{M}^\pm is given by

$$G_{\mu\nu;\alpha\beta}^\pm(z, z'; p^2) = G_h^\pm(z, z'; p^2) P_{\mu\nu;\alpha\beta}, \quad P_{\mu\nu;\alpha\beta} = g_{\mu\alpha}g_{\nu\beta} - \frac{1}{3}g_{\mu\nu}g_{\alpha\beta} + \mathcal{O}(p_\mu, \dots) \quad (\text{A.3})$$

where the $\mathcal{O}(p_\mu)$ terms vanish when $h_{\mu\nu}$ couples to an energy-momentum tensor that is conserved. This will be the case for the process considered here, for which the coupling is $M_5^{-3/2} h_{\mu\nu} T_{\text{SM}}^{\mu\nu}$. The scalar part of the 5D graviton propagator is given by¹⁰

$$G_h^+(z, z'; s) = -\frac{1}{C_h} \tilde{f}_+(z_<) \left(\tilde{f}_-(z_>) - \frac{f'_-(z_b)}{f'_+(z_b)} \tilde{f}_+(z_>) \right), \quad (\text{A.4})$$

$$G_h^-(z, z'; s) = -\frac{1}{C_h} \left(\tilde{f}_+(z_<) - \frac{f'_+(z_b)}{f'_-(z_b)} \tilde{f}_-(z_<) \right) \tilde{f}_-(z_>), \quad (\text{A.5})$$

where $\tilde{f}_\pm = e^{\pm m_g z \cdot \Delta}$ and $f_\pm = e^{m_g z} \tilde{f}_\pm$, while

$$\Delta = \sqrt{1 - \frac{s}{m_g^2}}, \quad (s \equiv -p^2), \quad (\text{A.6})$$

and the mass gap is given by

$$m_g = \frac{3}{2} \tilde{\eta}, \quad \text{with} \quad \tilde{\eta} = \eta \frac{r_b}{L}, \quad \eta = k e^{\tilde{v}_b}. \quad (\text{A.7})$$

We are using the notation $z_< = \min(z, z')$ and $z_> = \max(z, z')$. The C_h constant is fixed by the Wronskian of f_\pm in the form

$$C_h \equiv e^{-3A(z)} [f'_+(z)f_-(z) - f'_-(z)f_+(z)] = 2m_g \Delta, \quad (\text{A.8})$$

which turns out to be independent of z . Finally, the brane-to-brane propagator turns out to be

$$G_h^\pm(z_b, z_b; s) = -\frac{1}{m_g} \frac{1}{\Delta \pm 1}. \quad (\text{A.9})$$

Both \mathcal{M}^- and \mathcal{M}^+ spacetimes feature the same continuum of modes, starting at $m > m_g$. \mathcal{M}^- also have a massless mode corresponding to the physical graviton in 4D (this massless mode is absent in the \mathcal{M}^+). This can be seen by taking the limit of the propagator for

⁹The relation between conformal and brane cosmological coordinates is $z = -\frac{1}{\tilde{\eta}} \log(r/L)$, and the warp factor in conformal coordinates writes $A(z) = \tilde{\eta}z$. Further details on gauge fixing can be found in [6].

¹⁰The computation follows the same steps as in [70, 71]. See also [6, 72] for a computation of the propagator in the background with one brane and $\nu \neq 1$.

$s \rightarrow 0$, which gives

$$G_h^-(z_b, z_b; s) \underset{s \rightarrow 0}{\simeq} \frac{2m_g}{s}. \quad (\text{A.10})$$

We get $G_h^- \sim 1/s$, while for G_h^+ we get a constant behavior. This reproduces the results from [5].

In the following we consider only \mathcal{M}^- spacetime, hence we focus on the G_h^- propagator. The spectral function of this propagator is

$$\tilde{\rho}_h^-(s) \equiv -\frac{1}{\pi} \text{Im} G_h^-(z_b, z_b; s) = 2m_g \delta(s) + \frac{1}{\pi} \frac{\sqrt{s - m_g^2}}{s} \times \Theta(s - m_g^2). \quad (\text{A.11})$$

The massless graviton corresponds to the Dirac delta term.

A.2 Bulk Graviton Emission

The scattering amplitude of the graviton exchange process between SM fields $\varphi + \bar{\varphi} \rightarrow h_{\mu\nu}^* \rightarrow \varphi + \bar{\varphi}$ is given by

$$\mathcal{M}_{\varphi\varphi \rightarrow \varphi\varphi} = \langle 0 | h_{\mu\nu}(z_b, x) T_\varphi^{\mu\nu}(x) h_{\alpha\beta}(z_b, y) T_\varphi^{\alpha\beta}(y) | 0 \rangle. \quad (\text{A.12})$$

We write $\varphi = (s, f, V)$, with s for real scalars, f for Dirac fermions and V for real vectors.

We go to momentum space and focus on the exchange of the graviton continuum. The continuum propagator and corresponding spectral function are given by subtracting the zero mode as

$$G_h(z_b, z_b; s) \equiv G_h^-(z_b, z_b; s) - G_h^0(z_b, z_b; s) = \frac{m_g}{s} (\Delta - 1), \quad (\text{A.13})$$

$$\rho_h(s) \equiv \rho_h^-(s) - \rho_h^0(s) = \frac{1}{\pi} \frac{\sqrt{s - m_g^2}}{s} \Theta(s - m_g^2), \quad (\text{A.14})$$

where G_h^0 , ρ_h^0 , is the zero mode contribution in (A.10), (A.11).

The forward amplitude is written as

$$\begin{aligned} \mathcal{M}_{\varphi\varphi \rightarrow \varphi\varphi}^{\text{fw}} &\equiv \mathcal{M}(\varphi(p_1)\varphi(p_2) \rightarrow \varphi(p_1)\varphi(p_2)) = -\frac{1}{M_5^3} G_h(z_b, z_b; s) \times \mathcal{T}_\varphi, \\ \mathcal{T}_\varphi &\equiv \text{tr} T_\varphi^2 - \frac{1}{3} (\text{tr} T_\varphi)^2, \end{aligned} \quad (\text{A.15})$$

with $s = -(p_1 + p_2)^2$. We have used the identity $T_\varphi^{\mu\nu} P_{\mu\nu;\alpha\beta} T_\varphi^{\alpha\beta} = \text{tr} T_\varphi^2 - \frac{1}{3} (\text{tr} T_\varphi)^2$, neglected the mass of the SM particles, and averaged over initial state polarizations.

Finally we compute the total cross section for $\sigma(\varphi\varphi \rightarrow h_{\mu\nu})$ using the optical theorem, such that

$$\sigma_\varphi \equiv \sigma(\varphi\varphi \rightarrow h_{\mu\nu}) = \frac{1}{s} \text{Im} \mathcal{M}_{\varphi\varphi \rightarrow \varphi\varphi}^{\text{fw}}. \quad (\text{A.16})$$

Using Eq. (A.15) we obtain

$$\sigma_\varphi = \frac{1}{s} \frac{\sqrt{s - m_g^2}}{s} \Theta(s - m_g^2) \frac{\mathcal{T}_\varphi}{M_5^3} = \frac{c_\varphi}{M_5^3} \sqrt{s - m_g^2} \Theta(s - m_g^2), \quad (\text{A.17})$$

with

$$c_\varphi = (c_s, c_f, c_V) = \left(\frac{1}{12}, \frac{1}{16}, \frac{1}{4} \right). \quad (\text{A.18})$$

In the limit $s \gg m_g^2 \propto \eta^2$, the local curvature becomes negligible and the result agrees with the one from flat space [73].

The energy loss rate is then given by the interaction term of the Boltzmann equation, which can be directly written as

$$\Delta\dot{\rho}_{\text{SM}} = -\frac{1}{2} \sum_\varphi \kappa_\varphi^2 \int \frac{d^3 p_1}{(2\pi)^3} \frac{d^3 p_2}{(2\pi)^3} f_\varphi(E_1) f_\varphi(E_2) (E_1 + E_2) \sigma_\varphi v_{\text{rel}}, \quad (\text{A.19})$$

where $f_\varphi(E) = \frac{g_\varphi}{e^{E/T} \pm 1}$ is the thermal distribution for each of the SM fields with g_φ the multiplicity and κ_φ the number of spin degrees of freedom ($\kappa_s = 1$ and $\kappa_V = \kappa_f = 2$). This leads to (4.2).

References

- [1] S. Fichet, E. Megías, and M. Quirós, *Continuum effective field theories, gravity, and holography*, *Phys. Rev. D* **107** (2023), no. 9 096016, [[arXiv:2208.12273](#)].
- [2] S. Fichet, E. Megías, and M. Quirós, *Cosmological dark matter from a bulk black hole*, *Phys. Rev. D* **107** (2023), no. 11 115014, [[arXiv:2212.13268](#)].
- [3] O. Aharony, *A Brief review of 'little string theories'*, *Class. Quant. Grav.* **17** (2000) 929–938, [[hep-th/9911147](#)].
- [4] D. Kutasov, *Introduction to little string theory*, *ICTP Lect. Notes Ser.* **7** (2002) 165–209.
- [5] S. Fichet, E. Megías, and M. Quirós, *Holography of Linear Dilaton Spacetimes from the Bottom Up*, *Phys. Rev. D* **109** (2024), no. 10 106011, [[arXiv:2309.02489](#)].
- [6] S. Fichet, E. Megías, and M. Quirós, *Holographic fluids from 5D dilaton gravity*, *JHEP* **08** (2024) 077, [[arXiv:2311.14233](#)].
- [7] O. Aharony, M. Berkooz, D. Kutasov, and N. Seiberg, *Linear dilatons, NS five-branes and holography*, *JHEP* **10** (1998) 004, [[hep-th/9808149](#)].
- [8] E. Witten, *Anti-de Sitter space and holography*, *Adv. Theor. Math. Phys.* **2** (1998) 253–291, [[hep-th/9802150](#)].
- [9] S. S. Gubser, *AdS / CFT and gravity*, *Phys. Rev. D* **63** (2001) 084017, [[hep-th/9912001](#)].
- [10] J. M. Maldacena, *Eternal black holes in anti-de Sitter*, *JHEP* **04** (2003) 021, [[hep-th/0106112](#)].
- [11] L. Randall and R. Sundrum, *An Alternative to compactification*, *Phys. Rev. Lett.* **83** (1999) 4690–4693, [[hep-th/9906064](#)].

[12] P. Binetruy, C. Deffayet, U. Ellwanger, and D. Langlois, *Brane cosmological evolution in a bulk with cosmological constant*, *Phys. Lett. B* **477** (2000) 285–291, [[hep-th/9910219](#)].

[13] A. Hebecker and J. March-Russell, *Randall-Sundrum II cosmology, AdS / CFT, and the bulk black hole*, *Nucl. Phys. B* **608** (2001) 375–393, [[hep-ph/0103214](#)].

[14] D. Langlois, L. Sorbo, and M. Rodriguez-Martinez, *Cosmology of a brane radiating gravitons into the extra dimension*, *Phys. Rev. Lett.* **89** (2002) 171301, [[hep-th/0206146](#)].

[15] D. Langlois and L. Sorbo, *Bulk gravitons from a cosmological brane*, *Phys. Rev. D* **68** (2003) 084006, [[hep-th/0306281](#)].

[16] O. Trivedi and R. J. Scherrer, *Dark Matter from Holography*, [arXiv:2511.10617](#).

[17] G. 't Hooft, *Dimensional reduction in quantum gravity*, *Conf. Proc. C* **930308** (1993) 284–296, [[gr-qc/9310026](#)].

[18] L. Susskind, *The World as a hologram*, *J. Math. Phys.* **36** (1995) 6377–6396, [[hep-th/9409089](#)].

[19] G. 't Hooft, *The Holographic principle: Opening lecture*, *Subnucl. Ser.* **37** (2001) 72–100, [[hep-th/0003004](#)].

[20] R. Bousso, *A Covariant entropy conjecture*, *JHEP* **07** (1999) 004, [[hep-th/9905177](#)].

[21] R. Bousso, *The Holographic principle*, *Rev. Mod. Phys.* **74** (2002) 825–874, [[hep-th/0203101](#)].

[22] S. Fichet, *Shining Light on Polarizable Dark Particles*, *JHEP* **04** (2017) 088, [[arXiv:1609.01762](#)].

[23] K. R. Dienes, F. Huang, S. Su, and B. Thomas, *Dynamical Dark Matter from Strongly-Coupled Dark Sectors*, *Phys. Rev. D* **95** (2017), no. 4 043526, [[arXiv:1610.04112](#)].

[24] A. Mitridate, M. Redi, J. Smirnov, and A. Strumia, *Dark Matter as a weakly coupled Dark Baryon*, *JHEP* **10** (2017) 210, [[arXiv:1707.05380](#)].

[25] A. Francis, R. J. Hudspith, R. Lewis, and S. Tulin, *Dark Matter from Strong Dynamics: The Minimal Theory of Dark Baryons*, *JHEP* **12** (2018) 118, [[arXiv:1809.09117](#)].

[26] A. Batz, T. Cohen, D. Curtin, C. Gemmell, and G. D. Kribs, *Dark sector glueballs at the LHC*, *JHEP* **04** (2024) 070, [[arXiv:2310.13731](#)].

[27] K. Kong and K. T. Matchev, *Precise calculation of the relic density of Kaluza-Klein dark matter in universal extra dimensions*, *JHEP* **01** (2006) 038, [[hep-ph/0509119](#)].

[28] M. Kakizaki, S. Matsumoto, and M. Senami, *Relic abundance of dark matter in the minimal universal extra dimension model*, *Phys. Rev. D* **74** (2006) 023504, [[hep-ph/0605280](#)].

[29] N. R. Shah and C. E. M. Wagner, *Gravitons and dark matter in universal extra dimensions*, *Phys. Rev. D* **74** (2006) 104008, [[hep-ph/0608140](#)].

[30] D. Hooper and S. Profumo, *Dark Matter and Collider Phenomenology of Universal Extra Dimensions*, *Phys. Rept.* **453** (2007) 29–115, [[hep-ph/0701197](#)].

[31] G. Belanger, M. Kakizaki, and A. Pukhov, *Dark matter in UED: The Role of the second KK level*, *JCAP* **02** (2011) 009, [[arXiv:1012.2577](#)].

[32] P. Brax, S. Fichet, and P. Tanedo, *The Warped Dark Sector*, *Phys. Lett. B* **798** (2019) 135012, [[arXiv:1906.02199](#)].

[33] N. Bernal, A. Donini, M. G. Folgado, and N. Rius, *Kaluza-Klein FIMP Dark Matter in Warped Extra-Dimensions*, *JHEP* **09** (2020) 142, [[arXiv:2004.14403](https://arxiv.org/abs/2004.14403)].

[34] Y.-J. Kang and H. M. Lee, *Lightening Gravity-Mediated Dark Matter*, *Eur. Phys. J. C* **80** (2020), no. 7 602, [[arXiv:2001.04868](https://arxiv.org/abs/2001.04868)].

[35] Y.-J. Kang and H. M. Lee, *Dark matter self-interactions from spin-2 mediators*, *Eur. Phys. J. C* **81** (2021), no. 10 868, [[arXiv:2002.12779](https://arxiv.org/abs/2002.12779)].

[36] H. Cai, G. Cacciapaglia, and S. J. Lee, *Massive Gravitons as Feebly Interacting Dark Matter Candidates*, *Phys. Rev. Lett.* **128** (2022), no. 8 081806, [[arXiv:2107.14548](https://arxiv.org/abs/2107.14548)]. [Erratum: *Phys. Rev. Lett.* **132**, 169901 (2024)].

[37] C. Csaki, S. Hong, G. Kurup, S. J. Lee, M. Perelstein, and W. Xue, *Continuum dark matter*, *Phys. Rev. D* **105** (2022), no. 3 035025, [[arXiv:2105.07035](https://arxiv.org/abs/2105.07035)].

[38] W. D. Goldberger and I. Z. Rothstein, *High-energy field theory in truncated AdS backgrounds*, *Phys. Rev. Lett.* **89** (2002) 131601, [[hep-th/0204160](https://arxiv.org/abs/hep-th/0204160)].

[39] A. Costantino, S. Fichet, and P. Tanedo, *Effective Field Theory in AdS: Continuum Regime, Soft Bombs, and IR Emergence*, *Phys. Rev. D* **102** (2020), no. 11 115038, [[arXiv:2002.12335](https://arxiv.org/abs/2002.12335)].

[40] S. Ferrante, S. J. Lee, and M. Perelstein, *Collider signatures of near-continuum dark matter*, *JHEP* **05** (2024) 215, [[arXiv:2306.13009](https://arxiv.org/abs/2306.13009)].

[41] K. R. Dienes, S. Su, and B. Thomas, *Distinguishing Dynamical Dark Matter at the LHC*, *Phys. Rev. D* **86** (2012) 054008, [[arXiv:1204.4183](https://arxiv.org/abs/1204.4183)].

[42] C. Csaki, *TASI lectures on extra dimensions and branes*, in *From fields to strings: Circumnavigating theoretical physics. Ian Kogan memorial collection (3 volume set)*, pp. 605–698, 2004. [hep-ph/0404096](https://arxiv.org/abs/hep-ph/0404096). [,967(2004)].

[43] R. Sundrum, *Effective field theory for a three-brane universe*, *Phys. Rev. D* **59** (1999) 085009, [[hep-ph/9805471](https://arxiv.org/abs/hep-ph/9805471)].

[44] R. Sundrum, *Compactification for a three-brane universe*, *Phys. Rev. D* **59** (1999) 085010, [[hep-ph/9807348](https://arxiv.org/abs/hep-ph/9807348)].

[45] S. Barbosa, S. Fichet, E. Megías, and M. Quirós, *Entanglement entropy and thermal phase transitions from curvature singularities*, *JHEP* **04** (2025) 044, [[arXiv:2406.02899](https://arxiv.org/abs/2406.02899)].

[46] T. Shiromizu, K.-i. Maeda, and M. Sasaki, *The Einstein equation on the 3-brane world*, *Phys. Rev. D* **62** (2000) 024012, [[gr-qc/9910076](https://arxiv.org/abs/gr-qc/9910076)].

[47] D. Kutasov and D. A. Sahakyan, *Comments on the thermodynamics of little string theory*, *JHEP* **02** (2001) 021, [[hep-th/0012258](https://arxiv.org/abs/hep-th/0012258)].

[48] J. W. York, Jr., *Black hole thermodynamics and the Euclidean Einstein action*, *Phys. Rev. D* **33** (1986) 2092–2099.

[49] S. Hawking and D. N. Page, *Thermodynamics of Black Holes in anti-De Sitter Space*, *Commun. Math. Phys.* **87** (1983) 577.

[50] D. N. Page, *Thermal Stress Tensors in Static Einstein Spaces*, *Phys. Rev. D* **25** (1982) 1499.

[51] L. J. Hall, K. Jedamzik, J. March-Russell, and S. M. West, *Freeze-In Production of FIMP Dark Matter*, *JHEP* **03** (2010) 080, [[arXiv:0911.1120](https://arxiv.org/abs/0911.1120)].

[52] P. C. Vaidya, *Newtonian Time in General Relativity*, *Nature* **171** (1953) 260–261.

[53] R. W. Lindquist, R. A. Schwartz, and C. W. Misner, *Vaidya’s Radiating Schwarzschild Metric*, *Phys. Rev.* **137** (1965) B1364–B1368.

[54] S. W. Hawking, T. Hertog, and H. S. Reall, *Trace anomaly driven inflation*, *Phys. Rev. D* **63** (2001) 083504, [[hep-th/0010232](#)].

[55] J. L. Cook, E. Dimastrogiovanni, D. A. Easson, and L. M. Krauss, *Reheating predictions in single field inflation*, *JCAP* **04** (2015) 047, [[arXiv:1502.04673](#)].

[56] P. P. Avelino and V. M. C. Ferreira, *Constraints on the dark matter sound speed from galactic scales: the cases of the Modified and Extended Chaplygin Gas*, *Phys. Rev. D* **91** (2015), no. 8 083508, [[arXiv:1502.07583](#)].

[57] S. Hannestad, G. Raffelt, and Y. Y. Y. Wong, *Unparticle constraints from SN 1987A*, *Phys. Rev. D* **76** (2007) 121701, [[arXiv:0708.1404](#)].

[58] I. Lewis, *Cosmological and Astrophysical Constraints on Tensor Unparticles*, [arXiv:0710.4147](#).

[59] G. G. Raffelt, *Particle physics from stars*, *Ann. Rev. Nucl. Part. Sci.* **49** (1999) 163–216, [[hep-ph/9903472](#)].

[60] C. D. Hoyle, D. J. Kapner, B. R. Heckel, E. G. Adelberger, J. H. Gundlach, U. Schmidt, and H. E. Swanson, *Sub-millimeter tests of the gravitational inverse-square law*, *Phys. Rev. D* **70** (2004) 042004, [[hep-ph/0405262](#)].

[61] D. J. Kapner, T. S. Cook, E. G. Adelberger, J. H. Gundlach, B. R. Heckel, C. D. Hoyle, and H. E. Swanson, *Tests of the gravitational inverse-square law below the dark-energy length scale*, *Phys. Rev. Lett.* **98** (2007) 021101, [[hep-ph/0611184](#)].

[62] J. G. Lee, E. G. Adelberger, T. S. Cook, S. M. Fleischer, and B. R. Heckel, *New Test of the Gravitational $1/r^2$ Law at Separations down to $52 \mu\text{m}$* , *Phys. Rev. Lett.* **124** (2020), no. 10 101101, [[arXiv:2002.11761](#)].

[63] A. Costantino, S. Fichet, and P. Tanedo, *Exotic Spin-Dependent Forces from a Hidden Sector*, *JHEP* **03** (2020) 148, [[arXiv:1910.02972](#)].

[64] I. Chaffey, S. Fichet, and P. Tanedo, *Continuum-Mediated Self-Interacting Dark Matter*, *JHEP* **06** (2021) 008, [[arXiv:2102.05674](#)].

[65] P. F. de Salas, M. Lattanzi, G. Mangano, G. Miele, S. Pastor, and O. Pisanti, *Bounds on very low reheating scenarios after Planck*, *Phys. Rev. D* **92** (2015), no. 12 123534, [[arXiv:1511.00672](#)].

[66] C. Helsens, D. Jamin, M. L. Mangano, T. G. Rizzo, and M. Selvaggi, *Heavy resonances at energy-frontier hadron colliders*, *Eur. Phys. J. C* **79** (2019) 569, [[arXiv:1902.11217](#)].

[67] R. M. Harris, E. G. Guler, and Y. Guler, *Sensitivity to Dijet Resonances at Proton-Proton Colliders*, in *Snowmass 2021*, 2, 2022. [arXiv:2202.03389](#).

[68] D. C. Moore and A. A. Geraci, *Searching for new physics using optically levitated sensors*, *Quantum Sci. Technol.* **6** (2021), no. 1 014008, [[arXiv:2008.13197](#)].

[69] S. Fichet, E. Megías, M. Quirós, and G. Yamanaki, “Stable Black Strings from Warped Backgrounds.”

[70] S. Fichet, *Braneworld effective field theories — holography, consistency and conformal effects*, *JHEP* **04** (2020) 016, [[arXiv:1912.12316](#)].

- [71] E. Megías and M. Quirós, *The Continuum Linear Dilaton*, Acta Phys. Polon. B **52** (2021) 711, [[arXiv:2104.10260](https://arxiv.org/abs/2104.10260)].
- [72] S. Fichet, *On holography in general background and the boundary effective action from AdS to dS* , JHEP **07** (2022) 113, [[arXiv:2112.00746](https://arxiv.org/abs/2112.00746)].
- [73] G. F. Giudice, R. Rattazzi, and J. D. Wells, *Quantum gravity and extra dimensions at high-energy colliders*, Nucl. Phys. B **544** (1999) 3–38, [[hep-ph/9811291](https://arxiv.org/abs/hep-ph/9811291)].